TU Delft

Challenging Glass 2 – Conference on Architectural and Structural Applications of Glass, Bos, Louter, Veer (Eds.), TU Delft, May 2010.

Bonded Point-Supports: Understanding Today – Optimizing for the Future

Anneliese Hagl
Test+Ing Material GmbH, Germany, mail@test-ing-material.de

Experiments using material specimen of the Silicone adhesive on the one hand and several point support designs on the other hand provide valuable know-how for favourable layout from engineering point of view. The comparison of uni-axial material tests based on dog-bone specimens, of H-type specimens of ETAG 002 type and of circular and rectangular point supports show different working principles of the adhesive material. Test results on planar point supports and comparison with other point support designs show similarities in terms of applicable limit stresses. For advanced point support designs, these similarities might be affected by the support geometry leading to local stress peaks.

Keywords: Adhesive, Glass, Point support, Silicone, Structural Glazing

1. Introduction

Traditionally, Silicone adhesives are widely applied for line-type bonding geometries in structural glazing systems. Concerning the related designs, the adhesive material joints together the glass units of the glass façade with the supporting structure based on steel or Aluminum framework. Typical joint designs whose applications are regulated in depth in the European guideline ETAG 002 [1] are based on simple rectangular cross-section geometries. The ETAG 002 is focused only on a small range of bonding designs due to various limitations and simplifying assumptions e.g. two-sided line-type joints of moderate width to thickness ratios only. For approval of designs, special H-type specimens are defined within the ETAG 002 intended to simulate in experiments the line-type bonding designs of conventional structural glazing systems. Thus, the application of the ETAG 002 is based on extensive experimental campaigns and results under various operating conditions but does require little knowledge of the adhesive material itself.

Thus, it is not surprising that the application of bonded point supports is beyond the scope of the ETAG 002. Furthermore, the large variety of potential point support geometries result in more complex loading schemes of the adhesive material which is typically constraint by glass on the one hand and stainless steel or similar materials on the other hand. In case of tensile loading which is considered as the most critical load case, large interface areas of the adhesive to the adherents in combination with a small adhesive thickness in the range of some ‘mm’ lead to a significant suppression of lateral contraction of the adhesive. This effect is evoked by the much lower stiffness properties of the adhesive compared to the adherents, see Table 1. In addition, Silicone materials – almost incompressible as other elastomers – show a Poison’s ratio in the vicinity of 0.5 [2].

Table 1: Representative material properties.

Material	Young Modulus	Poison's Ratio	Density
Silicone	approx. 1 N/mm^2	approx. 0.5	1330 kg/m^3
Glass	70000 N/mm^2	0.23	2500 kg/m^3
Stainless Steel	170000 N/mm^2	0.3	7980 kg/m^3
Aluminium	70000 N/mm^2	0.3	2700 kg/m^3

The combination of these two topics – suppressed lateral contraction plus almost perfect incompressibility – leads to a complex material loading of the adhesive in case of tension forces acting on the point support. In the view of physical behaviour and mechanical performance, two issues are of high interest: strength and elasticity of the adhesive. Regarding strength properties of the applied Silicone [3], a straight forward approach is to compare dog-bone tests with experimental results of different kind of bonded point supports. In addition, results of an ETAG H-kind specimen are included as well. While the dog-bone and the ETAG specimen failures are of sudden nature, the fracture behaviour of the point supports featuring suppression of lateral contraction is more complex. Typically, the point supports show areas with different stiffness characteristics: high stiffness at the beginning and low stiffness afterwards. Examples for this special behaviour of point supports will be shown later in this paper, e.g. Figure 3.

For the case of sudden rupture experienced for dog-bone specimens and ETAG H-type specimens, limit loads before rupture are used for the entries in Table 2. In the case of circular and U-type point supports, Table 2 presents load levels related to significant stiffness changes. Please note that the loads F_R are normalized by the initial cross section A_0 leading to a significant deviation from true stresses especially for the dog bone specimen when large cross section area changes occur. In this case the true (or Cauchy) stress amounts up to 6 N/mm^2.

Table 2: Limit normal stresses (experimental results).

Specimen Type	Dog-bone Specimen	ETAG H-type Specimen	Circular Point Support	U-type Point Support
Geometry			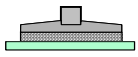	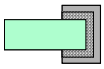
Stress F_R/A_0	1.9 N/mm²	1.1 N/mm²	0.9 N/mm²	1.2 N/mm²

The dog-bone specimen represents pure uni-axial loading of the adhesive. For the ETAG H-type specimen, non-uniform loading occurs due to the (stiff) plates built by glass, Aluminum or steel. For this geometry, high stress levels occur at the edges and in corners of the adhesive with the consequence of earlier failure compared to the dog-bone specimen with more homogenous material loading. The point supports differ from the dog-bone specimen by the complex loading of the adhesive due to suppressed lateral contraction leading to 3D stress states. Although the values of 0.9 N/mm^2 for a point support of 50 mm diameter and 1.2 N/mm^2 for the U-type support are not coincident at first glance, similarities will be discussed in the next paragraph. In addition it should be

noted that for the U-type point support the reference area A_0 is the frontal area defined by the glass thickness.

Table 3 compares strains and related flexibilities of the investigated specimens – this time based on numerical (Finite Element) models due to the difficulty of accurately measure compliances in complex test stands. It is obvious that the more the lateral suppression of the adhesive is constraint by the specimen geometry, the higher the effective stiffness is. Please note that the values might differ slightly depending on the chosen material law.

Table 3: Compliance properties (numerical results).

Nominal loading σ_N=1 N/mm^2	Dog-bone Specimen	ETAG H-type Specimen	Circular Point Support	U-type Point Support
Strain $\varepsilon_N=\Delta l/l_0$	1,19	0,82	0,08	0,06
Stiffness σ_N/ε_N	0,84	1,21	12,9	16,9
Stiffness related to dog-bone	1	1,44	15,4	20,1

Table 2 and Table 3 conclude that the behaviour of the adhesive must be seen with respect to its boundary conditions. Furthermore, the results motivate for more detailed investigations. The scope of bonded point supports might cover all designs with small sizes compared to the attached glass unit. Nevertheless, in this paper, focus is given on axial symmetric designs for simplicity.

2. Planar Point Supports

2.1. General

The most simple point support design consists in a planar point support bonded to the surface of the glass unit, see Figure 1. Typical loading schemes for point supports are shear loads, tensile loads and compression loads. Pure shear loads are reacted by the point support by the soft shear characteristics of the adhesive. The mechanical characteristics for this type of loading can be estimated by standard formula for elastic shear. In contrast, tensile and compression loads are more difficult to understand as highlighted in the paragraph before. As tensile loads are more critical e.g. wind suction loads of glass facades, focus in the paper will be given on this kind of loading.

For high accuracy of the bonding geometry activated by using special tools, both adherents of the specimens are built by steel fittings as shown in Figure 2. Comparisons with glass specimens do not show any noticeable differences, see also [4]. This behaviour is expected due to the very low stiffness of the adhesive compared to the adherents.

2.2. Experimental Results

Figure 3 presents the mechanical characteristics in terms of load versus deflection of a circular bond showing two representative curves. For deflections larger than 2 mm, the two curves significantly differ by the way of collapsing. In order to understand this behaviour, the specimens are shown in Figure 4. Obviously, flaws in the adhesive lead

to the differences in the results. Interestingly, the behaviour of the specimens up to 2 mm is in very good agreement in spite of the imperfections of the adhesive.

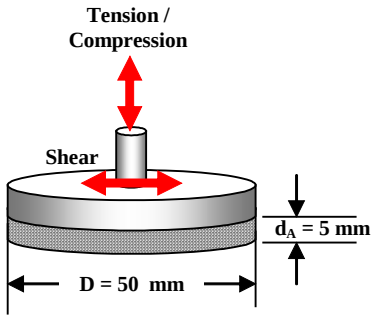

Figure 1: Point support geometry.

Figure 2: Photograph of point support specimen.

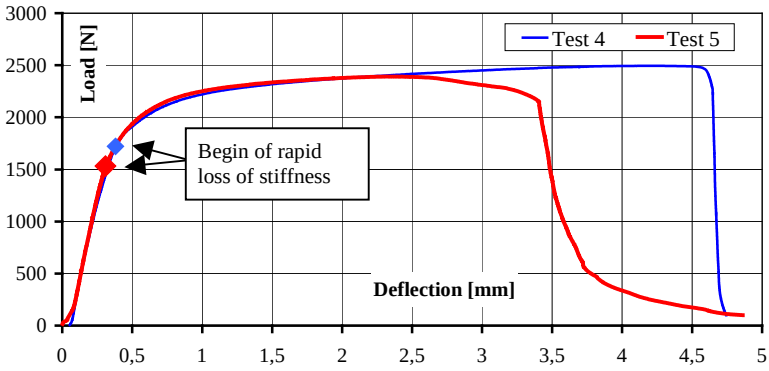

Figure 3: Test results for circular bonds of 50 mm diameter experiencing tensile loading.

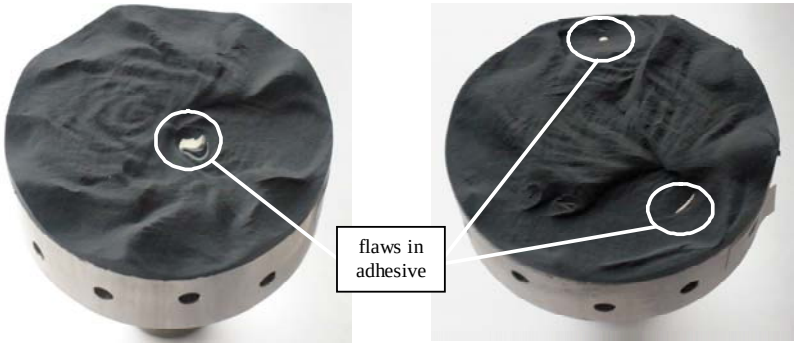

Figure 4: Specimens test 4 and 5.

In order to exploit the experimental data of Figure 3 in more detail, stiffness values are derived by numerical differentiation of the load versus deflection curve for test 5. The results shown in Figure 5 indicate a rapid loss of stiffness at a deflection of approximately 0.3 mm. The related data points are marked in Figure 3 for both tests. Obviously, these points are linked to the begin of adhesive damage.

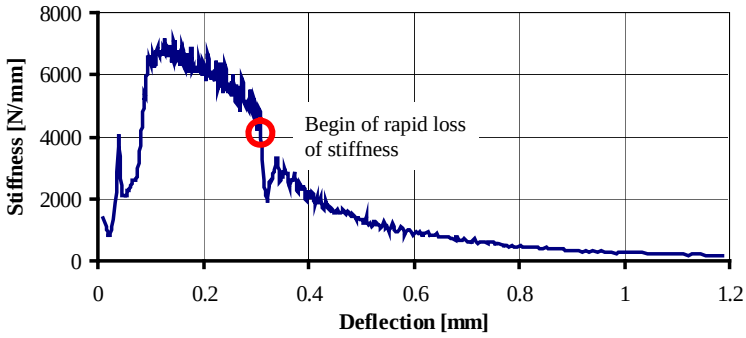

Figure 5: Specimen stiffness of test 5.

The following conclusions can be drawn from the experimental results:

- The curves can be divided into three partitions, the first partition ranging from start to approximately 1700 N, the second partition resembling a plateau area and the third partition with collapsing loads indicating the final break.
- Emphasized by the large gradient, the first partition refers to the elastic behaviour of the non-damaged point support. The agreement between the samples is very good until the mid of the second partition.
- The second partition is interpreted by first damages of the adhesive leading to the reduced effective stiffness of the point support. It is interesting to note that in this loading period, no cracks are visible from the outside of the specimen.
- The third partition is related to the total failure of the bond. Obviously, the start of this partition is triggered differently by imperfections in the adhesive.
- The area below the load versus deflection curve represents the energy absorbed by the point support. The observed behaviour is highly beneficial in terms of damage tolerance.

2.3. Numerical Results

Assuming that the begin of the break occurs when the stiffness of the point support significantly decreases, one obtains a load level of up to 1700 N for point supports of 50 mm diameter. Considering a cross section area of 1963 mm^2, the tensile force translates into an average tension stress level of 0.87 N/mm^2. Nevertheless, this simplified approach is only a very rough approximation of the real situation. Figure 6 presents a contour plot of the maximum principal stress distribution of the point support adhesive for a load level of 1700 N. Figure 7 shows the maximum stress distributions in radial direction for the element row at the interface to glass and steel respectively. The abscissa starts with r=0 in the center and is defined positive in radial direction. In

addition to the 50 mm diameter case, corresponding results are also presented for a point support of 70 mm diameter, see also [4].

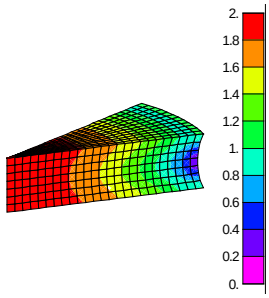

Figure 6: Maximum principal stresses of the point support model loaded by approx. 1700 N.

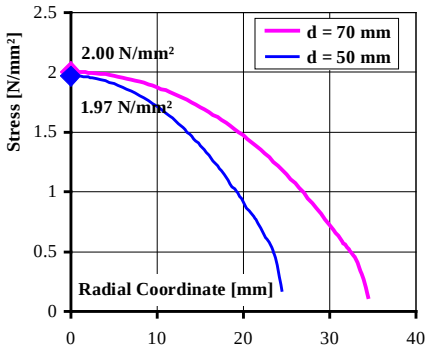

Figure 7: Comparison of maximum principal stresses for different point supports at beginning break.

It is interesting to note that in Figure 7 the maximum stress levels for both diameters achieve similar values in the center while the loading of the Finite Element models is based on experimental results referring to the begin of break. Values in the vicinity of 2 N/mm^2 are also known from other bonding geometries with highly suppressed lateral contraction such as the U-type bonding [5]. Thus, it can be assumed that this limit stress level is of more general validity for the investigated Silicone adhesive. Although the applicability of this approach is yet not fully explored with respect to potential limits, the assumption of approximately 2 N/mm^2 for begin of break is obviously an adequate starting point for the assessment of different point support designs.

3. Advanced Point Support Designs

For the usage of bonded point supports for laminated glass units, it is essential to adequately load all individual glass panes of the laminated glass. A straight forward approach is the jointing of the outer glass pane(s) with the point support via holes in the inner pane(s). In order to avoid unwanted loading of the PVB foil(s), a favourable point support design should aim on almost identical loading of the individual panes. In addition, it should be emphasized that the hereby achieved embedding of the point support into the inner glass pane leads especially to advantages for shear loading due to blockage effects. Please remember that for shear, no stiffening effects as for tensile loads can be activated by boundary conditions for planar point supports. Figure 8 presents an overview of point support designs of potential interest for a laminated glass unit featuring two panes.

The embedded point support ‘P0’ uses in principle the same design as a planar point support but features different boundary conditions. In order to increase the load share of the inner pane, the point support design ‘P1’ uses a conical design. Of course, the design space of the conical point support is constraint by assembly reasons. Thus, the minimum diameter of the hole in the glass must be larger than the maximum diameter of the support. The design ‘P2’ takes into account the idea that an increased bonding thickness in the center leads to an improved deformation pattern and thus to an

optimized load share between the two panes. Another approach is to apply an inner flange to the point support to be bonded to the inner pane as shown by the design ‘P3’.

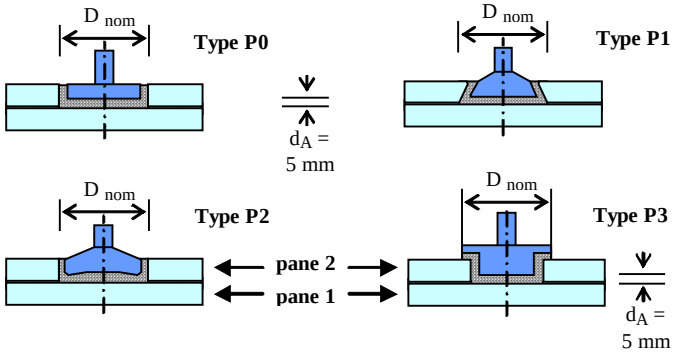

Figure 8: Overview of investigated point support designs.

Figure 9 presents the maximum principal stress distributions for the different point support designs under tension respecting the same maximum principal stress levels. Type ‘P1’ featuring the conical design was selected for an experimental campaign for checking the mechanical performance as this design is expected to show an interesting behaviour.

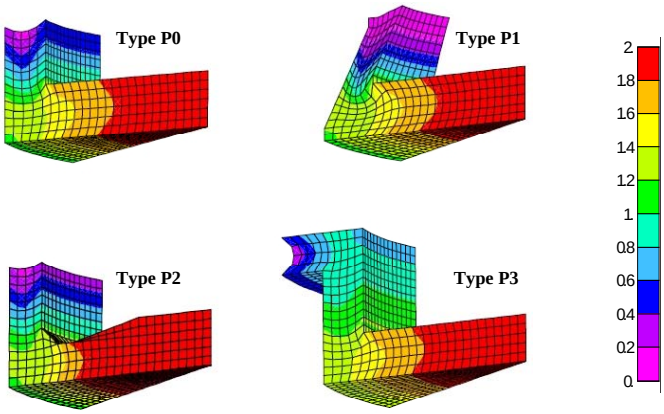

Figure 9: Maximum principal stresses for tensile loading.

4. Experiments for Advanced Point Support Type P1

4.1. Experimental Results for Type P1

Figure 10 gives an impression of the point support design P1 built by stainless steel while Figure 11 presents the test set-up in the testing machine. The experimental results are plotted in Figure 12 in terms of a load versus deflection graph. Compared to the planar point support, this point support shows very large deflections up to 10 mm and more before final failure. This behaviour is due to the conical shapes of the point

support and the adhesive providing additional resistance due to blockage before being pulled out. As in the case before, the analysis of the stiffness curve indicates the begin of failure in the point support, see Figure 13. Compared to the planar point support, the related load level is much lower, in the vicinity of 900 N.

Figure 10: Point support type P1.

Figure 11: Test set-up for point support P1.

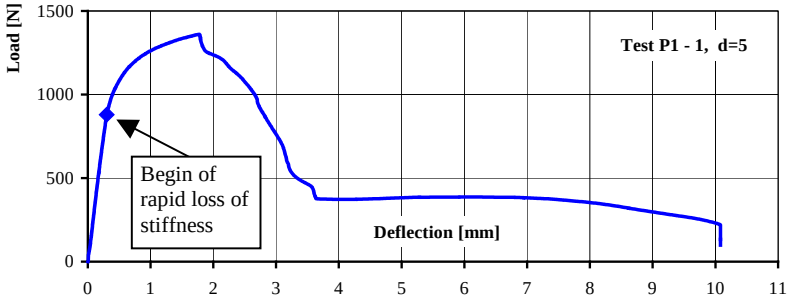

Figure 12: Test results for point support type P1.

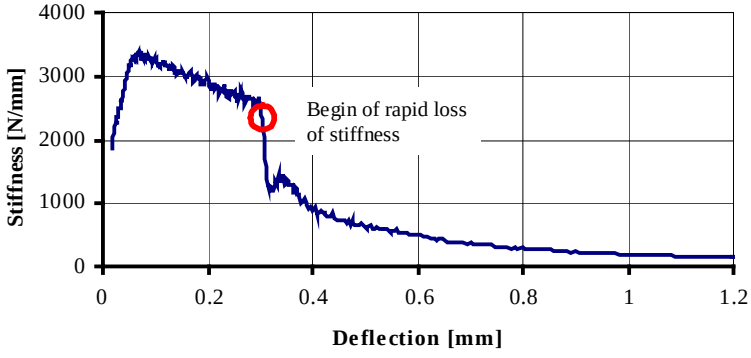

Figure 13: Specimen stiffness for point support type P1.

4.2. Assessment of the experimental results

The performance of the point support of type P1 was lower than originally expected. In order to understand this behaviour in more detail, a closer look was put on the broken specimen, see Figure 14. The photographs show that only the adhesive in the middle could be activated for load transfer. Based on these figures, the following hypothesis can be set up for point support P1: The circular edge of the point support enclosed by the front area and the cone – although smoothened by a radius – initiated a circular material failure in the point support due to high local stress levels, e.g. see maximum shear stress distribution in Figure 15. The expected cracks lead to a loading only below the point support front area which hereby acts similar as a planar point support of comparable diameter.

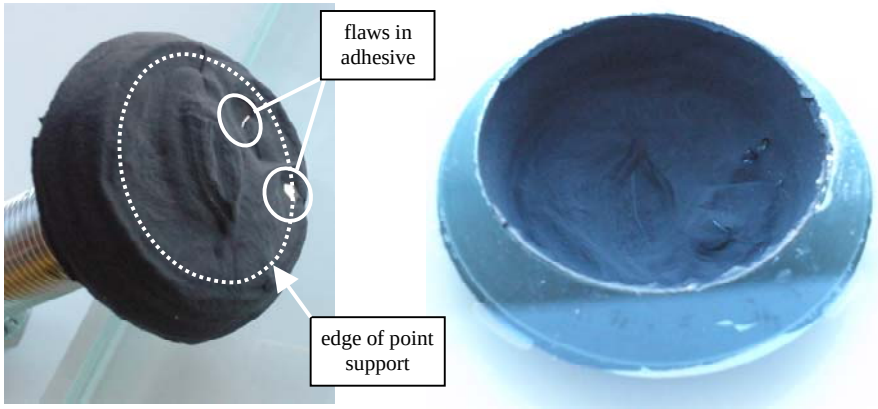

Figure 14: Specimen for point support type P1.

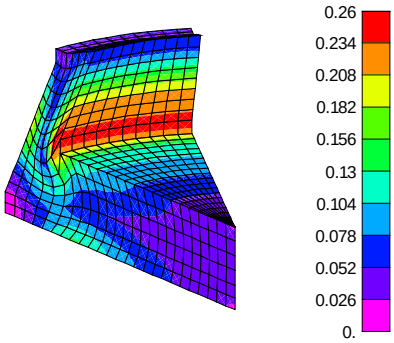

Figure 15: Maximum shear stress distribution for point support type P1.

Thus, the assumption of approximately 2 N/mm^2 is not fully valid for this kind of point support as the initial failure evoked by this special sharp design is not observed for conventional designs. If the impact of the initial failure is taken into account by only considering the adhesive material below the frontal area which is assumed to be somewhat cut out by cracks, the achieved load at begin of break can be explained by

comparing with planar point supports of similar frontal area – this time in coincidence with the 2 N/mm^2 level.

5. Conclusions

Comparisons of different specimens for Silicone adhesives show that the suppression of lateral contraction of the adhesive might alter the mechanical characteristics of the material significantly.
This effect is due to the low stiffness of the adhesive compared to materials like glass, steel and Aluminum on the one hand and due to the almost perfect incompressibility on the other hand.
For point supports, this effect might be dominant due to the small bonding thickness compared to the other sizes such as point support diameter or length and width.
For different point supports (e.g. circular planar supports, U-type supports), a maximum principal stress in the vicinity of 2 N/mm^2 is related to the limit loads before experiencing significant loss of stiffness.
For complex point support designs which might introduce local peaks in the adhesive loading e.g. by edges, a failure can occur before reaching this loading level.

6. Acknowledgements

The author would like to thank Glas Troesch preparing and providing the glass parts of the specimens for the advanced point support and Dow Corning GmbH, Germany, for performing the bonding of all needed specimens and the extensive support.

7. References

[1] NN, *ETAG 002 Guideline for European Technical Approval for Structural Sealant Glazing System (SSGS) - Part 1 Supported and unsupported systems*, www.eota.be/pdf/ssgs-fin-am3.pdf
[2] Wolf, A.T., Descamps, P., *Determination of Poisson's Ratio of Silicone Sealants from Ultrasonic and Tensile Measurements*, Performance of Exterior Building Walls, ASTM STP 1422, P.G. Johnson, Ed., American Society for Testing and Materials, West Conshohocken, PA, 2002
[3] Dow Corning., *Product Information*, Dow Corning ® 993
[4] Hagl, A., *Punktuelles Kleben mit Silikonen*, Stahlbau Vol.77, Issue 11, Ernst & Sohn Verlag, Berlin, Germany, 2008
[5] Hagl, A., *Understanding Complex Adhesive Behaviour: Case Study U-type Bonding Geometry*, Challenging Glass, Conference on Architectural and Structural Applications of Glass, May 2008, pp. 227 -240